

Equipartition and Transport in Two-Dimensional Electrostatic Turbulence

V. Naulin,¹ J. Nycander,² and J. Juul Rasmussen¹

¹Association EURATOM–Risø National Laboratory, Optics and Fluid Dynamics Department, OFD-128 Risø, 4000 Roskilde, Denmark

²Defence Research Establishment, Institute 64, 172 90 Stockholm, Sweden
(Received 15 September 1998)

Turbulent equipartition is investigated for the nonlinear evolution of pressure driven flute modes of a plasma in an inhomogeneous magnetic field. The Rayleigh-Taylor instability is recovered by linear stability analysis, and occurs when the pressure profile is more peaked than the profile of the magnetic field. Numerical solutions of the model equations on a bounded domain with sources and sinks show that the flux-driven turbulent fluctuations give rise to up-gradient transport, a “pinch flux,” of heat or particles. The averaged equilibrium density and temperature profiles approach $n \sim B$ and $T \sim B^{2/3}$, as predicted by turbulent equipartition. [S0031-9007(98)07538-3]

PACS numbers: 52.35.Py, 52.25.Fi, 52.35.Ra, 52.65.-y

Cross-field transport is one of the most important and most difficult areas of fusion research. Even basic transport phenomena such as profile resilience and the particle pinch, have no generally accepted explanations [1]. It is, however, recognized that low-frequency electrostatic turbulence accounts for the major part of the transport.

Whereas collisional transport is directed down-gradient, taking the plasma closer to the homogeneous thermal equilibrium, turbulent transport may be directed up-gradient. This is referred to as “pinch flux.” The particle pinch is well documented in tokamak plasmas [1] as the density peaks in the center, although the particle sources are usually situated near the wall. Also, the heat pinch has been demonstrated [2], and transient transport studies in particular provide clear evidence for nonlocal effects and up-gradient heat fluxes [3].

Recently, a new approach has been suggested for predicting the quasisteady profiles in tokamak plasmas [4–7]. It is based on the existence of Lagrangian invariants in the presence of turbulence. The basic assumption is that turbulent mixing causes equipartition of these invariants over the accessible phase space, a state denoted turbulent equipartition (TEP) [4]. Since the Lagrangian invariants depend on the magnetic field \mathbf{B} , a homogeneous distribution of these invariants implies that if \mathbf{B} is inhomogeneous so are the density and the temperature. Therefore, the fluxes that drive the plasma towards TEP may be up-gradient. Well-known cases of TEP occur in geophysical convection, as, for instance, in the troposphere, or in the convection zone of the sun (see, e.g., the discussion in Refs. [6,8]).

In a two-dimensional plasma model the corresponding mechanism is easily understood. If the magnetic field $\mathbf{B} = \hat{z}B(x, y)$ is inhomogeneous, the $\mathbf{E} \times \mathbf{B}$ drift $\mathbf{v}_E = (\hat{z} \times \nabla\phi)/B$ is compressible, and the relation $\nabla \cdot (B\mathbf{v}_E) = 0$ implies that n/B is a Lagrangian invariant. Another Lagrangian invariant is given by the specific entropy $T^{3/2}/n$. This gives the TEP profiles $n \sim B$ and $T \sim B^{2/3}$. If the diamagnetic drift $\mathbf{v}_d = -(\hat{z} \times \nabla p)/neB$ is also taken into account, these quantities are no longer exact

invariants; however, in the Rayleigh-Taylor instability (RTI), which generates the turbulence, the $\mathbf{E} \times \mathbf{B}$ drift dominates [9].

Previously, the TEP profile $n \sim B$ was obtained in a numerical experiment using random, externally imposed potential fluctuations, and only taking the $\mathbf{E} \times \mathbf{B}$ drift into account [10]. Here we present simulations of TEP with self-consistent, flux-driven electrostatic turbulence. The density and temperature profiles develop self-consistently under the influence of external heating.

A basic requirement of our model is that it must describe the fluid drifts accurately in the presence of an inhomogeneous magnetic field $\mathbf{B} = \hat{z}B(x, y)$. It must also describe the adiabatic compression and heating of a fluid parcel that is displaced into a region of larger B . (These requirements are not met in the commonly used flute mode models where the magnetic field inhomogeneity is represented by an “artificial gravity.”) We use the equations proposed by Isichenko and Yankov [11] for the electrons, together with the ion vorticity equation for cold ions. The system of equations is closed by assuming quasineutrality.

Briefly, the derivation is as follows. We use the drift approximation with typical frequencies much lower than the cyclotron frequencies, and neglect the electron inertia. Inserting the electron fluid velocity $\mathbf{v} = \mathbf{v}_E + \mathbf{v}_d$ into the continuity equation, $\partial n/\partial t + \nabla \cdot (n\mathbf{v}) = 0$, we obtain

$$\frac{\partial n}{\partial t} + \left\{ \phi, \frac{n}{B} \right\} - \left\{ p, \frac{1}{eB} \right\} = 0, \quad (1)$$

where the Poisson bracket is defined by $\{f, g\} = \partial_x f \partial_y g - \partial_x g \partial_y f$, e is the elementary charge, ϕ is the electrostatic potential, and the pressure is given by $p = nT$, with T the electron temperature. The third term in Eq. (1) comes from the diamagnetic drift.

The electron temperature equation is obtained from Braginskii’s transport equations [12] in the form $(3n/2)(\partial/\partial t + \mathbf{v} \cdot \nabla)T + nT\nabla \cdot \mathbf{v} = -\nabla \cdot \mathbf{q}$, where \mathbf{q} is the heat flux. Neglecting viscous effects, the

remaining diamagnetic part of \mathbf{q} can be written as $\mathbf{q} = -(5nT/2eB)\hat{z} \times \nabla T$. Using $\mathbf{v} = \mathbf{v}_E + \mathbf{v}_d$, we obtain

$$\frac{3}{2} \frac{\partial T}{\partial t} + \frac{1}{T^{1/2}} \left\{ \phi, \frac{T^{3/2}}{B} \right\} - \frac{1}{nT^{3/2}} \left\{ nT^{7/2}, \frac{1}{eB} \right\} = 0. \quad (2)$$

Equations (1) and (2) can also be obtained by taking moments of the gyrokinetic equation [11].

Because of the diamagnetic drift, neither of the quantities n/B or $T^{3/2}/n$ is an exact Lagrangian invariant of Eqs. (1) and (2). However, as shown in Ref. [11], there exist two other Lagrangian invariants $L_{\pm} = \pm(5/2)^{1/2} \ln(n/B) + \ln(T^{3/2}/n)$. They are advected with the velocities $\mathbf{v}_{\pm} = \mathbf{v} \mp (5/2)^{1/2} (1/eB)\hat{z} \times \nabla T$, which are neither fluid nor guiding center velocities. A spatially homogeneous distribution of L_+ and L_- gives

$$\frac{n(x, y)}{B(x, y)} = \text{const}, \quad \frac{T^{3/2}(x, y)}{B(x, y)} = \text{const}. \quad (3)$$

Hence, we expect the turbulence to drive the profiles toward those in Eq. (3).

In general, the $\mathbf{E} \times \mathbf{B}$ drift dominates in the linear RTI, for instance, both in the present model and in the rather different one considered in Ref. [9]. In this case, n/B and $T^{3/2}/n$ are approximate Lagrangian invariants, which again give the TEP profiles in Eq. (3). We therefore expect that these profiles apply to a broad class of flute mode models, even if they have no exact invariants corresponding to L_{\pm} .

Equations (1) and (2) govern the electron dynamics. To close the set of equations we use the quasineutrality condition ($n_e \approx n_i \approx n$) and the ion vorticity equation, obtained by taking the curl of the ion equation of motion. In the limit of cold ions, it reads $(d/dt)[(\omega + \omega_{ci})/n] = 0$. Here $d/dt = \partial/\partial t + \mathbf{v}_i \cdot \nabla$, $\hat{z}\omega = \nabla \times \mathbf{v}_i$ is the vorticity, and ω_{ci} is the ion cyclotron frequency. Considering the lowest order drift approximation, the ion velocity is simply given by the $\mathbf{E} \times \mathbf{B}$ drift, and $\omega = \nabla^2 \phi / B$. Also, using Eq. (1), we obtain

$$\frac{\partial \nabla^2 \phi}{\partial t} + \left\{ \phi, \frac{\nabla^2 \phi}{B} \right\} - \frac{eB^2}{m_i \mathcal{N}} \left\{ nT, \frac{1}{eB} \right\} = 0. \quad (4)$$

Here B and n are assumed to deviate only slightly from the constant reference levels \mathcal{B} and \mathcal{N} , to be introduced below.

Equations (1), (2), and (4) constitute a closed set of equations for low-frequency flute-type perturbations in a plasma with a nonuniform magnetic field. The equations conserve the energy

$$W = \int \left[\frac{m_i \mathcal{N}}{2\mathcal{B}^2} (\nabla \phi)^2 + \frac{3}{2} nT \right] dx dy, \quad (5)$$

which contains both kinetic and thermal energy.

To simplify the equations we will assume that the fields n , T , and B deviate only slightly from constant reference levels \mathcal{N} , \mathcal{T} , and \mathcal{B} , with, e.g., $n = \mathcal{N}[1 + \tilde{n}(x, y, t)]$

and similarly for temperature and magnetic field. Here \tilde{n} , \tilde{T} , and \tilde{B} are all of order $\epsilon \ll 1$. Inserting these expressions into Eqs. (1), (2), and (4), and keeping lowest order terms, we obtain

$$\frac{\partial n}{\partial t} + \{\phi, n - B\} + \{n + T, B\} = 0, \quad (6)$$

$$\frac{\partial T}{\partial t} + \left\{ \phi, T - \frac{2}{3} B \right\} + \left\{ \frac{2}{3} n + \frac{7}{3} T, B \right\} = 0, \quad (7)$$

$$\frac{\partial \nabla^2 \phi}{\partial t} + [\phi, \nabla^2 \phi] + [n + T, B] = 0. \quad (8)$$

For convenience we dropped the tilde. The potential is normalized by \mathcal{T}/e , the time by $\omega_{ci}^{-1} = m_i/eB$, and the space variables by $\rho = (\mathcal{T}/m_i)^{1/2}/\omega_{ci}$.

Equations (6) and (7) possess the Lagrangian invariants $I_{\pm} = \pm(5/2)^{1/2}(n - B) + 3T/2 - n$, corresponding to the invariants L_{\pm} of Eqs. (1) and (2). They are advected with the velocities $\mathbf{v}_{\pm} = \hat{z} \times \nabla \{\phi - n - [1 \pm (5/2)^{1/2}]T\}$. Thus, the TEP profiles are $n - B = \text{const}$ and $3T/2 - B = \text{const}$, corresponding to Eq. (3). Note that Eqs. (6)–(8) are scale invariant when B , n , and T are multiplied and t is divided by the same constant.

To lowest nontrivial order, and using mass conservation, the energy (5) in the fully nonlinear equations reduces to the heat $\int T dx dy$, which is trivially conserved according to Eq. (7). Equations (6)–(8) also conserve the energylike integral

$$E = \int \left[\frac{1}{2} (\nabla \phi)^2 + (n + T)B \right] dx dy. \quad (9)$$

The first term is the kinetic energy, while the second term has the form of potential energy. It represents the small part of the thermal energy which can be converted into kinetic energy when fluid parcels are displaced to a region with weaker magnetic field.

In order to investigate the linear stability we consider a slab model. We linearize Eqs. (6)–(8) around the background profiles $n_0(x)$, $T_0(x)$, and $B(x)$, and assume a waveform $\exp(i\mathbf{k} \cdot \mathbf{r} - i\omega t)$ in the local approximation. The dispersion relation reads

$$ck^2 \left[c^2 + \frac{10}{3} cB' + \frac{5}{3} (B')^2 \right] + cB' \left(n'_0 + T'_0 - \frac{5}{3} B' \right) + \frac{5}{3} (B')^2 (n'_0 - B') = 0, \quad (10)$$

where we have introduced $c = \omega/k_y$, and the prime denotes differentiation with respect to x . The long wavelength solution of the dispersion relation is $c^2 \approx -B'(n'_0 + T'_0 - \frac{5}{3} B')/k^2$. This is recognized as a special case of the RTI [9], with

$$B' \left(n'_0 + T'_0 - \frac{5}{3} B' \right) > 0, \quad (11)$$

as the condition for instability. The instability sets in if the pressure profile $n_0 + T_0$ is more peaked than $5B/3$.

Thus, the TEP profile $n - B = \text{const}$ and $T - 2B/3 = \text{const}$ is marginally stable. From Eq. (10) it is also seen that the RTI is stabilized at short wavelengths ($k \approx \rho^{-1}$) even though finite Larmor radius effects were not included, in contrast to conventional flute mode models employing an artificial gravity.

The quasilinear fluxes can be obtained as in Ref. [9], and we readily find that they are proportional to the gradients of the Lagrangian invariants: $\Gamma_n \propto -(n'_0 - B')$ and $q \propto -(T'_0 - 2B'/3)$. The energy flux is $Q_E \propto -(n'_0 + T'_0 - 5B'/3)$. Thus, the particle flux Γ_n can be negative if the density profile is flatter than B , and the heat flux q can be negative if the temperature profile is flatter than $2B/3$, while Q_E is always positive.

We have solved Eq. (6)–(8) numerically on a two-dimensional domain using a finite difference code. Dissipative terms of the form $\mu \nabla^2 f$, where f denotes n , T , or $\nabla^2 \phi$, were added to the right-hand side of each of the equations (6)–(8). The diffusivities μ were chosen to be of the order 10^{-3} . The computational domain was bounded in x and periodic in y , with the size $L_x = 5$ and $L_y = 20$. By prescribing $\partial_x n|_{x=\pm L_x/2} = 0$ the diffusive particle flux at the walls was set to zero. The potential ϕ was kept constant at the walls so that the velocity component perpendicular to the walls, and, consequently, the turbulent fluxes at the walls, vanished.

In the first experiment the turbulence is driven by a distributed heat source in a region near $x = 0$, while the temperature at both boundaries is fixed to zero. The magnetic field is of the form $B \sim 1/(3.5 + x)$ and the system is initialized with uniform profiles $n = T = 0$ and low amplitude random noise. The system starts to heat up and, as predicted, a RTI sets in. After a few hundred time units, large convective cells appear, in addition

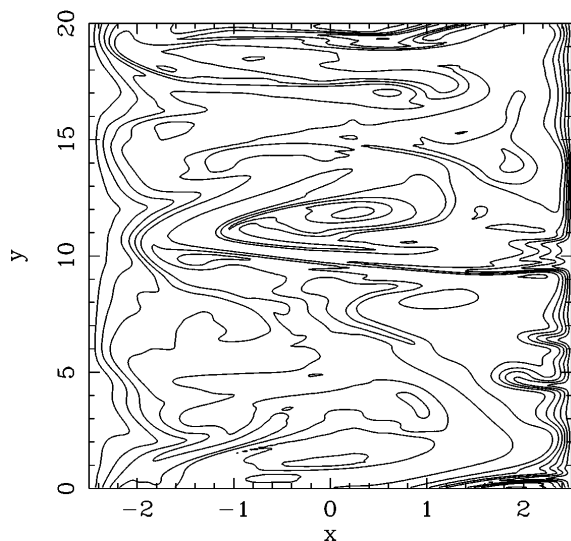


FIG. 1. Isocontours of the temperature in the saturated state. The system is heated at about $x = 0$ (see Fig. 2). Spacing between contours is $\Delta T = 1$.

to the small scale turbulence (Fig. 1), and a statistical equilibrium is approached. The unidirectional spectrum of, e.g., the squared potential fluctuations reveals a power law behavior $k^{-\alpha}$ with $\alpha \approx 2$, and with the maximum amplitude at the largest wavelength that fits into the domain. Note that in this situation no inertial range is expected as the driving can be active on all scales. Near the walls the heat flux is purely diffusive, while strong turbulent mixing is the dominant transport mechanism in the interior region, and there we expect TEP. In Fig. 2 we show the temperature (with temporal evolution) and the density profile averaged over y and 50 time units in the equilibrium state. Both approach the TEP profiles in the quasistationary limit. Note that the RTI initially develops only to the right of the heat source (shaded in Fig. 2), in accordance with the stability criterion (11). During the nonlinear stage the turbulence spreads leftward, and the temperature maximum is then found to the left of the heat source. Thus, there is an up-gradient heat flux in the region $-1.5 > x > -0.2$.

In the second experiment, the turbulence is driven by an imposed temperature difference between the walls, using $T|_{x=-L_x/2} = 10$ and $T|_{x=+L_x/2} = 0$. The magnetic

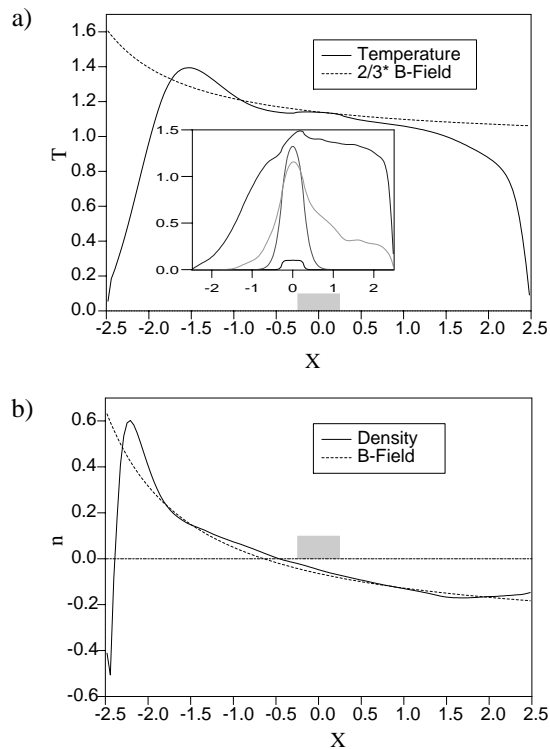


FIG. 2. Temperature (a) and density (b) profiles with TEP prediction ($T - 2/3 B = \text{const}$ and $n - B = \text{const}$) when the system is heated in the shaded area. The magnetic field is given by $B = 1/(3.5 + x)$. The temperature maximum is to the left of the heated area, demonstrating the heat pinch. The leftward heat flux from the source to the wall at $x = -2.5$ is about 25% of the total heating. The inset in (a) shows the temperature profile at times 2, 30, 70, and 250. Note that the RTI operates only to the right initially.

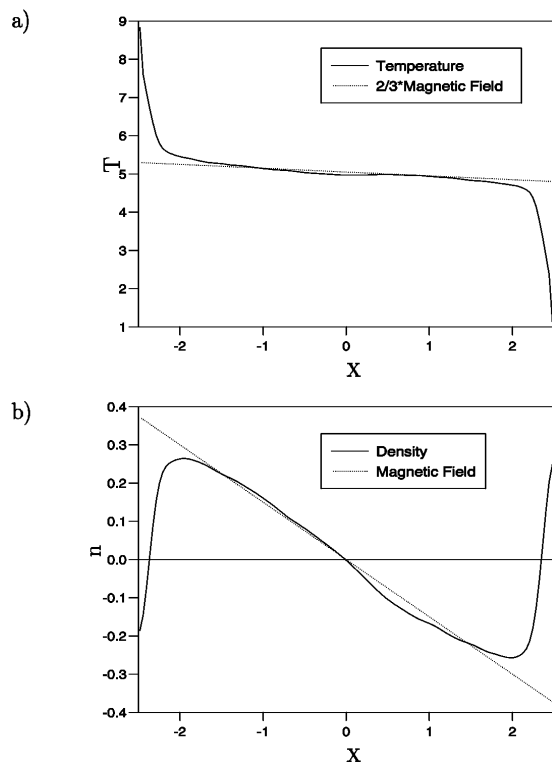


FIG. 3. Temperature (a) and density (b) profiles and TEP prediction ($T - 2/3B = \text{const}$ and $n - B = \text{const}$). The turbulence is driven by prescribing $T(-2.5) = 10$ and $T(2.5) = 0$ at the boundaries.

field is $B(x) = -0.15x$. The temperature fluctuations reach values of the order of the boundary temperature, while the density and potential fluctuations are much smaller. As seen from Fig. 3, the temperature and density profiles away from the diffusive boundary layers agree very well with the TEP predictions $T - 2B/3 = \text{const}$ and $n - B = \text{const}$. A change of the diffusivities μ changes the size of the boundary layers and fluxes, while the profiles in the central region remain unchanged. Note that particles are transported leftward as the density gradient develops, revealing the presence of a transient particle pinch. A steady-state particle pinch is impossible *a priori* in this experiment, since the setup guarantees that the equilibrium particle flux vanishes. However, when we change the boundary conditions to allow particles to diffuse across the boundaries at $x = \pm L_x/2$, a leftward pinch flux appears.

If the imposed temperature difference between the walls is increased, most of the additional temperature drop occurs over the diffusive boundary layers, while the profile stays approximately the same in the central region. This is an example of profile resilience.

We have also considered other situations, and, in general, find that the plasma relaxes toward the TEP profiles if the aspect ratio of the box $L_y/L_x > 2$. For a smaller aspect ratio, a zonal flow corresponding to a

y -independent potential appears. This may be described as a tendency for the ion potential vorticity $\nabla^2\phi + B - n$ to be uniformly distributed. Detailed investigations of this point and the influence of a shear flow on the TEP evolution, as well as details on the developing turbulence, will be presented in a forthcoming paper.

In conclusion, we verified that the nonlinear evolution of pressure driven electrostatic flute modes in a system with sources and sinks leads to a quasiequilibrium with density and temperature profiles as predicted by the TEP, i.e., with the Lagrangian invariants n/B and $T^{3/2}/B$ roughly constant. The instability gives rise to pinch fluxes of heat and particles into the region with a stronger magnetic field. The physical mechanism of these fluxes is the adiabatic compression of fluid parcels as they are displaced into this region. The turbulent fluxes are proportional to the gradients of n/B and $T^{3/2}/B$, rather than to the gradients of the density and temperature themselves.

The results indicate that TEP profiles may also be the turbulent attractors in more complex and realistic models for toroidal plasma devices, which, however, should include the trapped particles [6].

We thank K. Rypdal and V. V. Yankov for useful and constructive discussions. This work was partly supported by the Danish Natural Sciences Foundation (SNF Grant No. 9600852). One of us (V.N.) was supported by Marie Curie Grant No. 5004-CT96-5023.

-
- [1] F. Wagner and U. Stroth, *Plasma Phys. Control. Fusion* **35**, 1321 (1993).
 - [2] C. C. Petty and T. C. Luce, *Nucl. Fusion* **30**, 121 (1994).
 - [3] J. D. Callen and M. W. Kissick, *Plasma Phys. Control. Fusion* **39**, B173 (1997).
 - [4] V. V. Yankov, *JETP Lett.* **60**, 171 (1994).
 - [5] J. Nycander and V. V. Yankov, *Phys. Plasmas* **2**, 2874 (1995).
 - [6] V. V. Yankov and J. Nycander, *Phys. Plasmas* **4**, 2907 (1997).
 - [7] M. B. Isichenko, A. V. Gruzinov, and P. Diamond, *Phys. Rev. Lett.* **74**, 4436 (1995); M. B. Isichenko, A. V. Gruzinov, P. Diamond, and P. N. Yushmanov, *Phys. Plasmas* **3**, 1916 (1996).
 - [8] J. Nycander and V. V. Yankov, *Phys. Scr.* **T63**, 174 (1996).
 - [9] J. Nycander and J. Juul Rasmussen, *Plasma Phys. Control. Fusion* **39**, 1861 (1997).
 - [10] M. B. Isichenko and N. V. Petviashvili, *Phys. Plasmas* **2**, 3650 (1995).
 - [11] M. B. Isichenko and V. V. Yankov, *Phys. Rep.* **283**, 161 (1997).
 - [12] S. I. Braginskii *Reviews of Plasma Physics*, edited by M. A. Leontovich (Consultants Bureau, New York, 1965), Vol. 1, p. 205.